Study on sound absorption behavior of multi-component polyester nonwovens: experimental and numerical methods

Tao Yang[1], Ferina Saati[2], Kirill V Horoshenkov[3], Xiaoman Xiong[1], Kai Yang[1], Rajesh Mishra[1], Steffen Marburg[2] and Jiří Militký[1]

[1]*Department of Material Engineering, Faculty of Textile Engineering, Technical University of Liberec, Liberec 46117, Czech Republic*

[2]*Vibroacoustics of Vehicles and Machines, Technical University of Munich, Boltzmannstrasse 15, 85748 Garching, Germany*

[3]*Department of Mechanical Engineering, The University of Sheffield, Sheffield S1 3JD, United Kingdom*

Abstract:

This study presents an investigation of the acoustical properties of multi-component polyester nonwovens with experimental and numerical methods. 15 types of nonwoven samples made with staple, hollow and bi-component polyester fibers were chosen to carry out this study. The AFD300 AcoustiFlow device was employed to measure airflow resistivity. Several models were grouped in theoretical and empirical model categories and used to predict the airflow resistivity. A simple empirical model based on fiber diameter and fabric bulk density was obtained through power-fitting method. The difference between measured and predicted airflow resistivity was analyzed. The surface impedance and sound absorption coefficient were determined by using 45mm Materiacustica impedance tube. Some widely used impedance models were used to predict acoustical properties. Comparison between measured and predicted values was carried out to determine the most accurate model for multi-component polyester nonwovens. The results show that one of the Tarnow model provides the closest prediction to the measured value with an error of 12%. The proposed power-fitted empirical model exhibits very small error of 6.8%. It is shown that the Delany-Bazley and Miki models can accurately predict surface impedance of multi-component polyester nonwovens, but Komatsu model is less especially at the low-frequency range. The results indicate that the Miki model is the most accurate method to predict the sound absorption coefficient with mean error of 8.39%.

Keywords

polyester, nonwoven, airflow resistivity, impedance, sound absorption, models

Introduction

Porous sound absorbers are widely used to reduce noise and to control reverberation time. Energy loss caused by viscous effects and thermal losses are primarily the mechanism involved in sound absorption by porous materials.[1] Such losses occur during sound propagation in the interconnected pores of a porous absorbent. A thin layer of air adjacent to the wall of a pore is where viscous losses happen. This is due to viscosity of air so sound dissipates with friction between the pore walls. Thermal conductivity of the air and the absorbent material has some impact on losses as well, often being more important at low frequencies. Sound energy losses due to vibrations of the material also happen, but they are usually less important than the viscous-thermal absorption effects as sound propagates mainly through the interconnected pores which volume prevail. Fibrous materials are typical porous materials, playing an important role in building and automotive industries for noise control and sound quality. Due to their high porosity, low pollution, light weight, low cost and high absorbing, fibrous materials are popular sounds absorbers.[2]

The noise reduction application of inorganic fibrous materials, such as glass fiber and mineral wool, attracted a considerable attention due to their large specific surface area and high acoustical performance. The characteristic impedance and sound absorption of glass fiber and mineral wool have been investigated using impedance tube and Johnson-Champoux-Allard (JCA) model in Wang and Torng's study.[3] They stated that the difference in sound absorption is not obvious for materials with different bulk densities. Chen and Jiang[4] compared the sound absorption of activated carbon fiber and glass fiber separately laminated with pure cotton, pure ramie and pure polypropylene (PP) nonwovens. Their results indicated that nonwovens with activated carbon fiber as surface layer have better sound absorption than nonwovens with surface layer of glass fiber. Although inorganic fibrous materials have significant advantages, there are potential human health problems as a result of inhaling fibers or due to skin irritation and lay-down in the lung alveoli.[5] Thus, some researchers investigate the usage of natural fibers instead of inorganic fibers.

Compared to glass fiber and mineral wool, natural fibers as sound-absorbing materials have relatively high thermal and acoustic performances and are more environmentally friendly. Reviews of acoustic properties of natural fibers can be found in literature.[6-7] The sound absorption and physical properties of nonwovens produced via needle-punching through combining banana, bamboo and jute fibers with PP staple fibers have been reported in the ratio of 50 : 50.[8] The results showed that bamboo/PP nonwoven exhibits higher stiffness, better sound absorption, higher tensile strength, lower elongation, lower thermal conductivity and lower air permeability. It is known to be more suitable for interior automotive noise control than other fiber composites. Oldham et al.[9] carried out experiments for sound absorption on cotton, wool, ramie, flax, jute and sisal fiber through impedance tube and reverberation chamber measurements. They studied the accuracy of the Delany-Bazely and Garai-Pompoli models for the prediction of the absorptive properties of natural fibers. They stated that the two prediction models agree with measured data for natural fibers with less than 60 μm diameter. However, these models have less than satisfactory applicability in the case of most natural fibers where fiber diameters are relatively large.

Beside inorganic and natural fibers, synthetic fibers presently play an important role in applications for noise reduction. Unlike natural fibers, synthetic fibrous materials can be more widely used in various applications for noise reduction due to their structural diversity. Pelegrinis et al.[10] applied an alternative model based on the Kozeny-Carman equation, to theoretically predict the airflow resistivity of polyester materials with uniform fiber diameter. The airflow resistivity retrieved using the Miki model applied to absorption coefficient data was compared with the predicted airflow resistivity. The results indicated that the flow resistivity retrieved from the acoustical absorption data agreed well with that predicted by the Kozeny-Carman model, giving an error within 10%. The thermal properties and sound absorption of high-loft nonwovens made by staple, hollow and bi-component polyester were reported in refs. [11,12] The results showed that high-loft polyester nonwovens result in a sound absorption that shows a strong correlation with their thermal resistance. In addition, it was concluded that polyester nonwovens show the best sound absorption performance with airflow resistivity of 6000 Pa s/m^2. An investigation by Tascan and Vaughn[13] into the acoustical insulation of different types of polyester fiber was also carried out. In this work it was stated that materials with 3-denier fibers were better sound insulators than the ones with 15-denier fibers. It also indicated that 4DG and trilobal polyester fibers have better sound insulation results than nonwoven fabrics made from round fibers.

Although a number of studies related to the acoustic properties of fibrous materials have been reported, there are only a few publications focusing on multi-component polyester nonwovens. [14] Thus, the aim of the current study is to investigate the airflow resistivity, impedance and sound absorption of multi-component polyester nonwovens by using practical measurements and existing prediction methods. The accuracy between measured and predicted results is analyzed.

Some models for airflow resistivity and impedance prediction

The presently widely used sound absorption prediction methods are based on the theory proposed by Zwikker and Kosten.[15] In their theory, the surface characteristic impedance of rigidly-backed layer of porous material with finite thickness can be calculated from the following equation:

$$Z_s = Z_c \coth(kl)\ , \tag{1}$$

where Z_s is the surface characteristic impedance, Z_c is the characteristic impedance, k is the propagation constant and l is the material thickness. Then, the normal-incidence sound absorption coefficient can be derived from the surface characteristic impedance as

$$\alpha = 1 - |R|^2 = 1 - \left| \frac{\frac{Z_s}{\rho_0 c_0} - 1}{\frac{Z_s}{\rho_0 c_0} + 1} \right|^2 , \tag{2}$$

where α is the sound absorption coefficient, R is the pressure reflection coefficient, ρ_0 is the air density at room temperature, and c_0 is the sound speed in air media at room temperature.

Airflow resistivity models

In a majority of the impedance models, the airflow resistivity is the critical parameter to predict the characteristic impedance and propagation constant. The airflow resistivity is a measure of how easy air passes through a porous absorber and the resistance that airflow meets through a structure. This measure gives an estimate of the sound energy penetrated in the material pores and lost due to inertia and viscous effects in the pore structure. Therefore, the airflow resistivity is very important parameter to determine accurately. Xue et al.[14] proposed a modification based on the existing models for two-component fibrous materials with varying fiber diameter. In their paper, the micro-CT measurement was applied to obtain the fiber radii distribution. By applying the fiber radii distribution in one of the Tarnow model, they accurately predicted the airflow resistivity of materials having two fiber components. Models for predicting the airflow resistivity by using bulk density, porosity and mean fiber diameter are available.[16] Existing models can be categorized into two groups: theoretical and empirical models. A summary of some commonly used theoretical and empirical models is given in Table 1.

The theoretical models for airflow resistivity are mainly based on two theories: drag force theory and capillary channel theory. The capillary channel theory assumes that the flow through the porous material is treated as a conduit flow between cylindrical parallel capillary tubes.[17] The flow resistivity theoretically related to the material bulk density, fiber diameter and porosity as suggested by Carman and Kozeny.[17] Pelegrinis et al.[10] modified the Kozeny-Carmen model to predict more accurately the airflow resistivity of uniform fiber diameter polyester material. In drag force theory, the fibers in the porous material, or in other words the walls of the pores in the structure are treated as obstacles to an otherwise straight flow of the fluid and the fibers cannot be displaced.[18] Drag force theory models demonstrate the relationship between permeability and the internal structural architecture of the porous material unlike capillary flow theory. Langmuir developed the earliest equivalent dimensionless permeability for flow parallel to an array.[19] A new way to calculate the airflow resistivity of randomly placed parallel fibers based on Voronoi polygons was presented by Tarnow.[20] He proposed a two-dimensional model that consists of parallel fibers randomly spaced for flow perpendicular to, or parallel with the fibers. Since samples in this study have perpendicular-laid fiber structure, one of the Tarnow's models used to predict airflow parallel passing through fibers arranged in random lattice is listed in Table 1.

The empirical airflow resistivity model was first introduced by Nichols, which requires an adjustable parameter $0.3 \leq x \leq 1$.[21] Nichols model was modified by Garai and Pompoli[22] for accurate prediction of airflow resistivity for double-fiber component polyester materials. Manning and Panneton[23] established three simple airflow resistivity models based on weight of evidence approach for Shoddy fiber materials which were manufactured by three different bonding methods. Thermal bonding material model was selected due to that the chosen high-loft nonwovens were thermally bonded. The applied fiber diameter determination method in this study is different with Xue's method[14] because the fiber components used in our research have various length. The fiber diameter was calculated by using length-weighted average method, detailed method will be introduced in the Materials section.

Table 1. Some airflow resistivity models established using theoretical and empirical methods.

Category	Model	Airflow resistivity
Capillary channel theory	Kozeny-Carman[17]	$\sigma = \frac{180\eta(1-\varepsilon)^2}{d^2\varepsilon^3}$
	Pelegrinis et al.[10]	$\sigma = \frac{180\eta(1-\varepsilon)^2}{d^2}$
Drag force theory	Langmuir[19]	$\sigma = \frac{16\eta(1-\varepsilon)}{d^2[-\ln(1-\varepsilon) - 1.5 + 2(1-\varepsilon) - \frac{(1-\varepsilon)^2}{2}]}$
	Tarnow[20]	Airflow is parallel to fibers arranged in random lattice $\sigma = \frac{16\eta(1-\varepsilon)}{d^2[-1.280\ln(1-\varepsilon) + 0.526 - 2\varepsilon]}$
Empirical Method	Garai-Pompoli[22]	$\sigma = \frac{2.83\times10^{-8}\times\rho^{1.404}}{d^2}$
	Manning-Panneton[23]	Thermal bonded $\sigma = \frac{1.94\times10^{-8}\times\rho^{1.516}}{d^2}$

Note: σ is the airflow resistivity, η is the dynamic viscosity of air, ε is the material porosity and d is the fiber diameter.

Impedance models

When modelling the acoustical behavior of porous materials, non-acoustic parameters such as porosity, airflow resistivity, tortuosity, thermal permeability and viscous and thermal characteristic lengths are difficult to determine. Therefore, usage of empirical models that are developed by regression method based on a reduced set of non-acoustical parameters is more popular. As described with Eqs. (1) and (2), it is essential to obtain the characteristic impedance and propagation constant to predict the surface characteristic impedance and sound absorption coefficient. Therefore, several impedance models are introduced in this section. The summary of the formula for these impedance models are presented in Appendix A.

Delany-Bazley model

Delany and Bazley[24] carried out several impedance tube measurements in the 1960s with which they could derive empirical relationships between impedance and propagation constant to the airflow resistivity (see Eqs. (A1) and (A2) in Appendix A). These relationships are widely used across quite a wide frequency range due to the reasonable estimations. It is necessary to note that several empirical models have been developed based on Delany-Bazley model. In Delany-

Bazley model,[24] only a non-acoustical parameter of airflow resistivity is required to predict acoustical characteristics.

Miki model

Miki[25] developed a new regression model based on experimental data from Delany and Bazley's study in 1989. Miki proposed modifications to the Delany-Bazley model were in order to generate a more accurate model, valid for a broader frequency range (see Eqs. (A3) and (4) in Appendix A).

Garai-Pompoli model

A new simple model for airflow resistivity prediction which was developed by Garai and Pompoli. They also presented a modified impedance model based on Delany-Bazley method (see Eqs. (A5) and (A6) in Appendix A).[22] The accuracy of Delany-Bazley, Dunn-Davern and Garai-Pompoli prediction models were investigated by comparing the measured sound absorption of polyester materials with diameter ranging from18 to 48 μm[22], suggesting a suitable method of prediction for the acoustical characteristics of polyester materials. They performed a similar set of measurements on polyester materials to those of Delany-Bazely's.

Komatsu model

Komatsu[26] proposed a new prediction model (Eqs. (A7) and (A8) in Appendix A) based on the impedance tube measurements from 15 types of glass fiber and 9 types of mineral wool samples in 2008. The airflow resistivity of the samples ranges from 6000 to 72900 Pa·s/m^2. He stated that this new model was more accurate for the prediction of the acoustical properties of a fibrous material when compared with the Delany-Bazley and Miki models.

Materials and methods

Materials

In this study, three samples were selected. First, a polyester nonwoven sample was produced using vibrating perpendicular technology. In addition, two commercially available types of polyester nonwoven materials that were made separately using rotation-vibration perpendicular technology.[12, 27] Sample WM20 was prepared using perpendicular rotation technology; samples STG1 and STG2 were produced using perpendicular vibration technology. The fiber content in all of the samples in this study was the same. The sheath part of bi-component fibers was low-melting polyethylene terephthalate (PET). Three types of polyester fiber exist in the polyester materials. In order to get the cross-sectional slice of fibers, the resin embedding

technology was utilized. Cross sectional and longitudinal microscopic images were also captured (see in Figure 1) at the Technical University of Liberec using JENAPOL microscope and NIS-elements software.

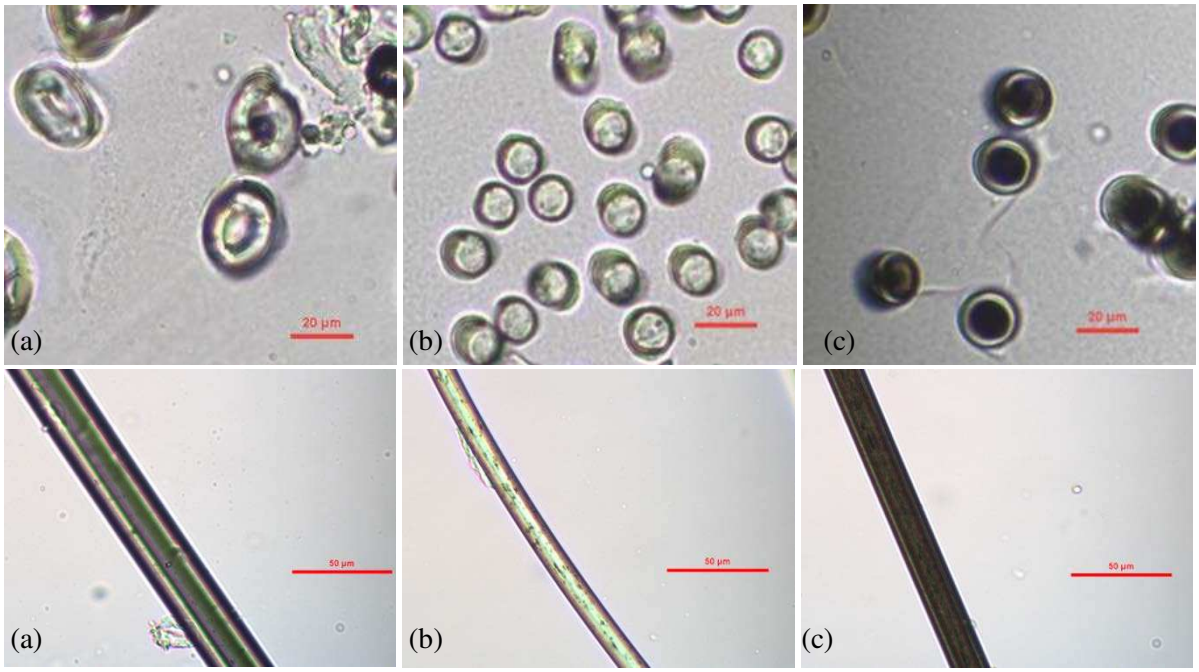

Figure 1. Cross-sectional and longitudinal microscopic images of polyester fibers: (a) hollow PET; (b) PET; (c) bi-component PET.

Table 2. Key characteristics of polyester materials used in this study.

Samples	Fiber contents	Mean fiber diameter (μm)	Porosity (%)	Bulk density (kg/m^3)	Thickness (mm)	Surface density (g/m^2)	Airflow resistivity (Pa·s/m²)	Fiber orientation angle (°)
WM20	30% - Hollow PET	15.94	98.15	21.07	24.09	507.5	5757 ± 589	56.07
WM20			97.86	24.45	20.76	507.5	7319 ± 243	45.65
WM20			97.66	26.71	19.00	507.5	7530 ± 408	40.88
WM20	45% - PET		97.59	27.54	18.43	507.5	9829 ± 376	39.41
WM20			96.89	35.56	14.27	507.5	14989 ± 285	29.44
WM20	25% - Bi-component PET		96.86	35.87	14.15	507.5	15414 ± 167	29.17
WM20			96.01	45.56	11.14	507.5	19733 ± 433	22.56
ST G1			97.94	23.54	20.32	478.3	7498 ± 332	45.70

ST G1	97.29	30.94	15.46	478.3	13397 ± 277	32.99
ST G2	98.52	16.93	27.48	465.2	4108 ± 199	79.09
ST G2	98.29	19.49	23.87	465.2	5337 ± 217	58.53
ST G2	98.03	22.48	20.69	465.2	7029 ± 356	47.67
ST G2	97.58	27.61	16.85	465.2	10181 ± 259	37.02
ST G2	96.94	34.95	13.31	465.2	12868 ± 199	28.40
ST G2	96.09	44.60	10.43	465.2	20474 ± 687	21.88

To prepare polyester nonwoven samples with various densities and thicknesses, heat pressing method was used. Samples WM20, ST G1, and ST G2 got compressed under 600 Pa pressure at 130 ℃ for the duration of 5 minutes. Thickness gauges were used to ensure the specific thickness attained at the end of this process. In Table 2, the characteristics of the polyester specimens are listed. The content percentage of samples is based on weight. The mean fiber diameter is length weighted average value as defined in Eq. (3). Reproducible statistics were ensured through 250 fiber diameter measurements for each type of fiber. According to ASTM C830-00, sample porosities were determined[28] as $\varepsilon = 1 - \rho/\rho_f$, where ρ_f is the fiber density that was 1141.82 kg/m^3 for the fiber material used in this study, and ρ is the fabric bulk density. The densities of the three fiber types were measured by liquid pycnometer method.[29] Since the closed pores have little or no effect on the airflow resistivity and sound absorption, voids in hollow fibers were not included in this analysis.[30] By means of an Alambeta device (SENSORA), fabric thicknesses were measured and fabric surface density was determined according to ISO 9073-1:1989.[31] Figure 2 illustrates that the majority of fibers in an uncompressed sample are vertically orientated and parallel arranged. The fiber orientation angle in this study (Figure 2, areas highlighted in red) was defined as the angle between the surface of the material specimen and the dominant fiber axis. Such an angle is dependent on material density or compression degree of the fibrous specimen. During the process of heat press, the angle of fiber orientation decreased and consequently, thickness of specimen reduced and material density increased.

$$d = d_i \frac{l_i}{\sum_{i=1}^{N} l_i} + d_{i+1} \frac{l_{i+1}}{\sum_{i=1}^{N} l_i} + \cdots + d_N \frac{l_N}{\sum_{i=1}^{N} l_i}, \quad (3)$$

where d_i is the fiber diameter obtained from average value of 50 fibers, and l_i is the total fiber length for each type fiber in a unit volume of nonwoven fabric:

$$l_i = \frac{W_i}{\pi (d_i/2)^2 \rho_i}, \quad (4)$$

where W_i is the fiber total weight in a unit volume of nonwoven fabric, and ρ_i is the fiber density.

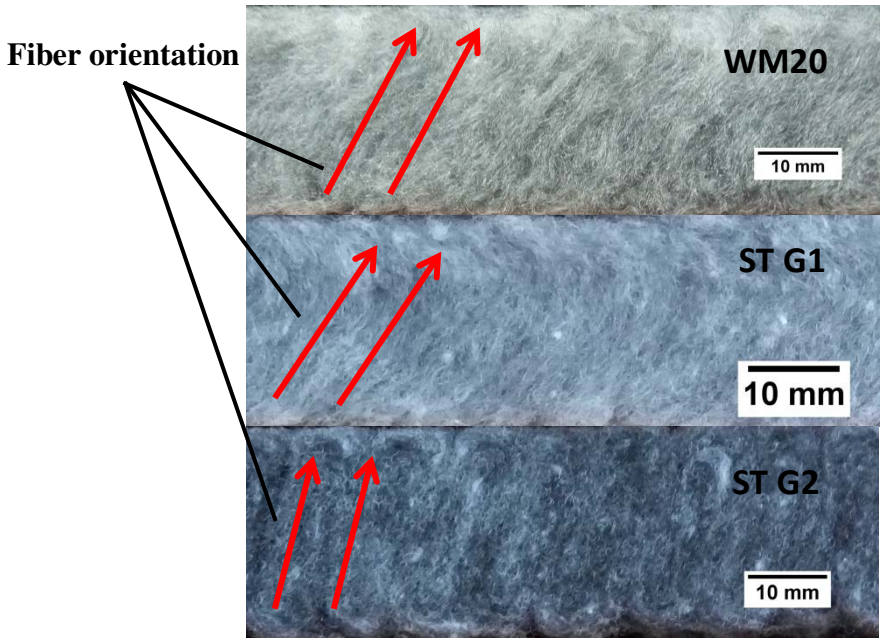

Figure 2. Cross-sectional macroscopic images of samples WM20, ST G1 and ST G2.

Circular specimens with 100mm diameter were cut with an ELEKTRONISCHE STANZMASCHINE TYPE 208. Measurements were carried out in a standard setup for air flow resistivity. In current study, the airflow resistivity was measured directly with an AFD300 AcoustiFlow device (Gesellschaft für Akustikforschung Dresden mbH, Dresden, Germany) according to ISO 9053:1991.[32] The AcoustiFlow device determines the airflow resistivity based on direct-airflow method on open porosity porous materials. For each polyester nonwoven fabric, ten samples were measured to ensure the reproducibility of the airflow resistivity experiment, results summarized in Table 2.

Impedance tube measurement

Acoustic properties of materials can be evaluated by steady-state methods, reverberant chamber methods, impedance tube methods, etc. In this study, the impedance tube was used to obtain normal incidence impedance. The surface impedance of polyester nonwovens was determined according to ISO 10534-2.[33] The 45 mm impedance tube manufactured by Materiacustica was used to carry out the impedance measurements. The measurement frequency range was between 200 and 4200 Hz. The lower boundary was chosen higher than the tube limit in order to avoid inaccuracies caused by structural vibrations or phase mismatch.[34] The measurements of airflow resistivity and impedance were carried in the Jonas Lab at the University of Sheffield. For each nonwoven fabric, ten samples were measured.

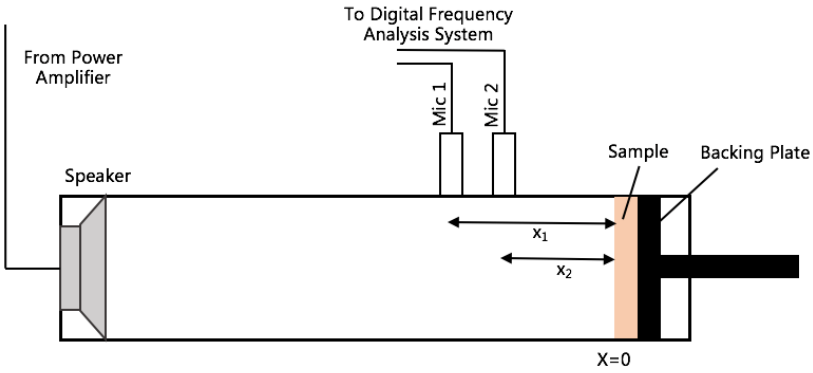

Figure 3. Two-microphone impedance tube schematic.

A schematic of the two microphone impedance tube setup used in this work is depicted in Figure 3. Steady state pressure in the impedance tube is given by:

$$p = A(e^{kx} + Re^{-kx}) \,, \tag{5}$$

where *A* is a complex constant, *R* is the pressure reflection coefficient, *k* is the propagation constant, and *x* is the position of sample surface in the tube.

There are two standard methods for sampling the pressure within the tube: standing wave ratio method and transfer function technique.[1] The second method was applied for determination of impedance in this work. The transfer function between two microphone positions in the impedance tube is measured as shown in Figure 3. The transfer function is the ratio of pressure between two microphone positions:

$$H_{12} = \frac{p_{x2}}{p_{x1}} \,, \tag{6}$$

and then using Eq. (5), the transfer function is given by:

$$H_{12} = \frac{e^{kx_2} + Re^{-kx_2}}{e^{kx_1} + Re^{-kx_1}} \,, \tag{7}$$

where $x_1$and x_2 are the positions of the microphones as shown in Figure 3. From Eq. (7), the complex pressure reflection coefficient can be obtained by:

$$R = \frac{H_{12}e^{kx_1} - e^{kx_2}}{e^{-kx_2} - H_{12}e^{-kx_1}} \,. \tag{8}$$

Appling Eq. (8) to Eq. (2), the surface impedance and sound absorption coefficient are consequently attained.

Results and Discussion

The predicted and measured impedance, airflow resistivity and sound absorption coefficient of multi-component polyester nonwovens were presented in this section. The accuracy of

impedance and airflow resistivity models was investigated, comparing the relative prediction errors.

Airflow resistivity

In order to investigate the accuracy of airflow resistivity models, the relative errors, δ, between predicted and measured data were calculated according to the following equation:

$$\delta = \frac{\sum_{i=1}^{N} \delta_i}{N} = \frac{1}{N} \sum_{i=1}^{N} \frac{|\sigma_{m,i} - \sigma_{p,i}|}{\sigma_{m,i}} \times 100\% \,, \tag{9}$$

where σ_m is the measured airflow resistivity, σ_p is the predicted airflow resistivity, and N is number of the tested configurations (N=15).

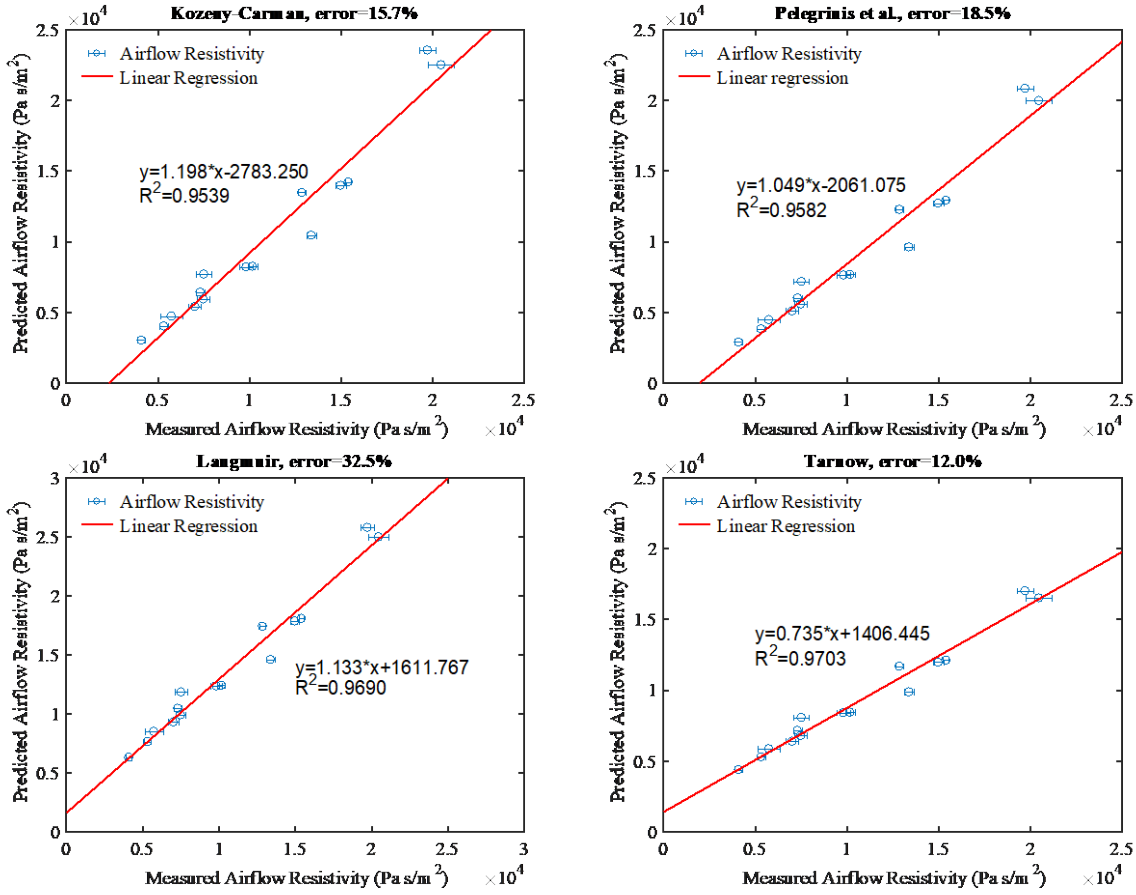

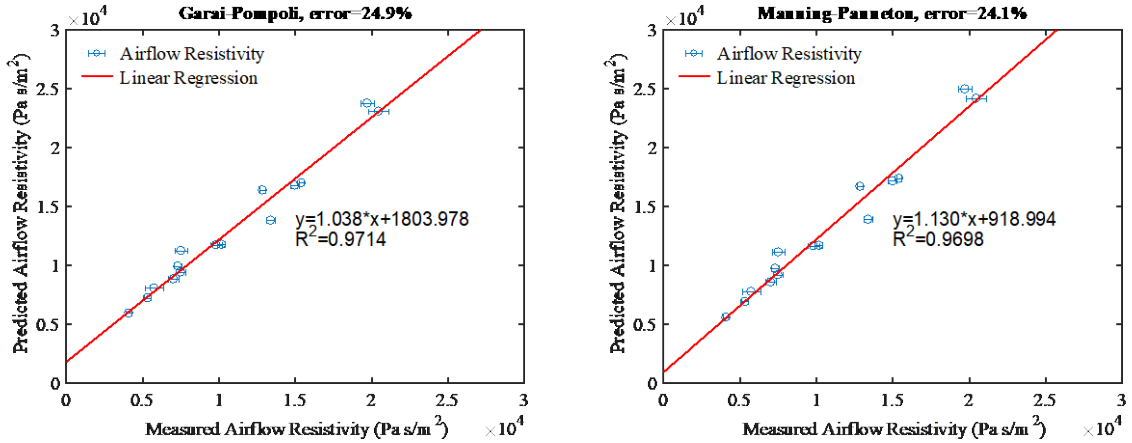

Figure 4. The prediction error of airflow resistivity and the linear relation between measured and predicted airflow resistivity.

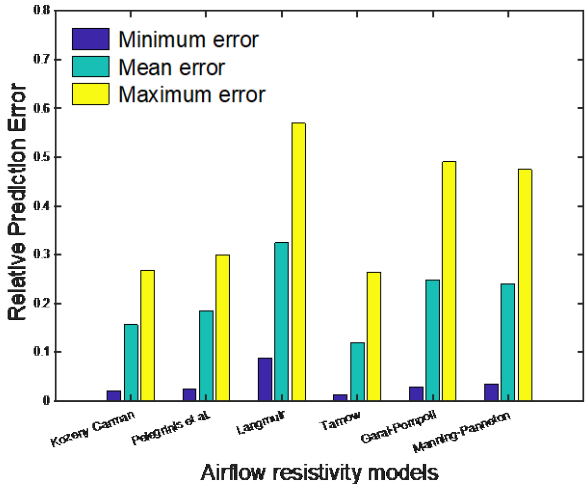

Figure 5. The minimum, mean and maximum prediction error based on some airflow resistivity models. The mean error δ was obtained using Eq. (9).

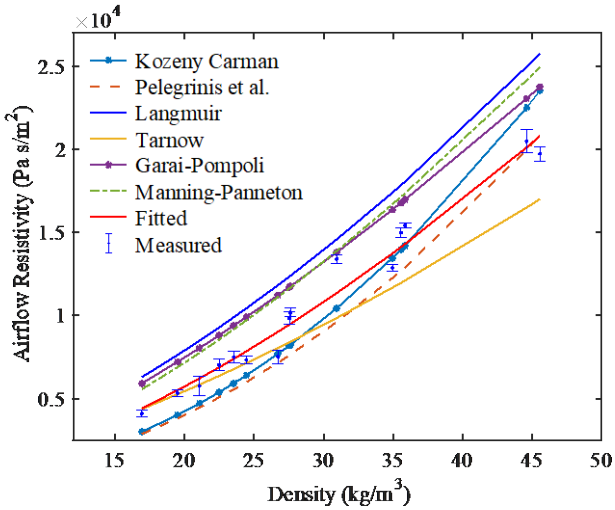

Figure 6. Predicted airflow resistivity and fitted model.

Figure 4 presents the comparison of the predicted airflow resistivity values against the measured values. The minimum, mean and maximum prediction errors among the polyester nonwoven samples are shown in Figure 5. The predicted airflow resistivity values based on theoretical and empirical models are shown in Figure 6 as a function of the bulk density. It is observed that the relative prediction error lies in the range of 12-32.5%. It can be found that the minimum and maximum errors have same trend with mean relative errors from Figure 5. In the three groups of prediction models, the capillary channel theory models (Kozeny-Carman and Pelegrinis *et al*) exhibit relatively low errors between 15.7% and 18.5%. A similar error among capillary channel theory models is due to that the Pelegrinis *et al* model was slightly modified from Kozeny-Carmen model. However, Pelegrinis *et al* model shows better prediction for denser samples (e.g. > 35 kg/m^3), although Kozeny-Carman model has better accuracy. Figure 6 shows that the model developed by Langmuir significantly overestimates the resistivity. Therefore, Langmuir model exhibits the highest relative error with a value of 32.5%. The most accurate model for the airflow resistivity of multi component polyester nonwovens is the Tarnow model that is accurate within 12%. Furthermore, when materials are of relatively lower density, the Tarnow model gives a higher accuracy, whereas this model exhibits higher variation compared to measured values at high density range. To explain this phenomenon, fiber orientation angle was decreased with the increase in the density for high specimen compression as illustrated in Figure 2 and Table 2. Reduction in the fiber orientation angle leads to the airflow no longer be parallel to the fibers. As the orientation angle approaches 0, the airflow becomes perpendicular to the fibers. For compressed materials, the measured airflow resistivity (see Figure 6) is higher than that predicted by Tarnow model which works better when flow is parallel to the fibers. It can be concluded that Tarnow model is more accurate for multi-component polyester with lower density and airflow resistivity. For the samples with denser structure and lower airflow resistivity, Pelegrinis et al. model is more accurate. The Garai-Pompoli and Manning-Panneton models predict similar values of airflow resistivity. The linear regression between measured and predicted value is also presented in Figure 4. It can be seen that all the regression lines have slope values close to 1 except Tarnow

method. This is because of the fact that the predicted airflow resistivity by Tarnow model for denser samples is relatively low compared with measured value. The coefficient of determinations for the models are over 0.95.

Although one drag force theory model exhibits acceptable accuracy for multi-component polyester nonwovens, the two empirical models are not reliable which overestimate the airflow resistivity by 24%. One same type simple empirical model was developed by power-fitting the values of measured resistivity, the model presented in Eq. (10). The fitted empirical model is show in Figure 6. The relative prediction error of the fitted empirical model is 6.8%. The values of predicted airflow resistivity for each sample are presented in Appendix B. It was similar to that adopted in ref. [34].

$$\sigma = \frac{1.3395\times10^{-8}\times\rho^{1.565}}{d^2} \quad . \tag{10}$$

Surface impedance and absorption coefficient

The effect of a porous surface on the incident acoustic wave can be characterized by four interrelated acoustic quantities: impedance, admittance, pressure reflection coefficient and absorption coefficient. The impedance, admittance and pressure reflection coefficient describe the magnitude and phase change in the wave upon reflection. The absorption coefficient only gives information about the energy change on reflection.[15] The impedance models introduced in previous section were used to predict characteristic impedance and propagation constant. By substituting the characteristic impedance and propagation constant into Eqs. (1) and (2), the surface impedance and sound absorption can be easily obtained. The surface impedance contains real part (resistance) and imaginary part (reactance). The real part of surface impedance is associated with energy propagated in the material, and the imaginary part with phase changes. Thus, the surface acoustic impedance gives more insight information about the absorbing properties of a material than the absorption coefficient. The predicted surface impedance and absorption coefficient will be demonstrated in this section. In addition, the accuracy between predicted and measured absorption coefficient will be presented.

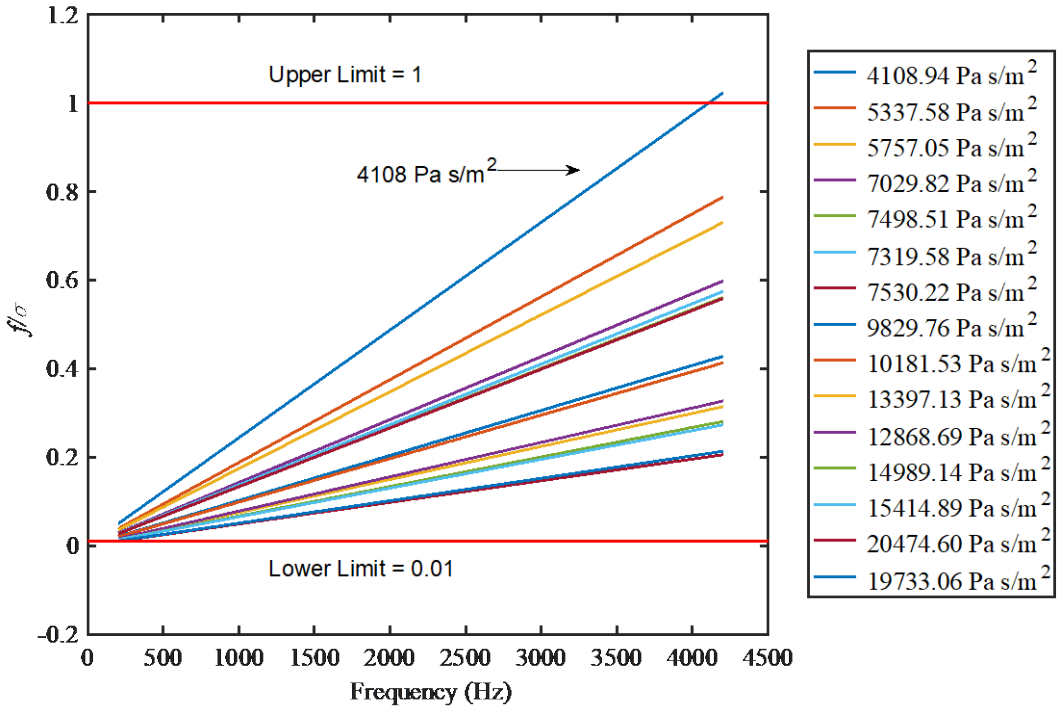

Figure 7. Range of the ratio of frequency to airflow resistivity of nonwoven samples. The lower and upper limits are shown in terms of the applicability of the Delany and Bazley model.

Delany and Bazley advised that their method is more accurate in the range of $10^{-2} \leq \frac{f}{\sigma} \leq 1$.[23] In order to verify the adaptability of Delany-Bazley model for predicting impedance and sound absorption of multi-component polyester nonwovens, the $\frac{f}{\sigma}$ against frequency has been presented in Figure 7 for the materials considered in this study. The slope of each line is equal to the reciprocal of airflow resistivity (σ). It can be seen that one sample with 4108 Pa s/m² airflow resistivity demonstrates high value of $\frac{f}{\sigma}$ (i.e. > 1) from 4108 to 4200 Hz which means the sample with lowest airflow resistivity has 2.3% invalid prediction range in the whole measurement range (200 - 4200 Hz). Miki, Garai and Komatsu stated that their methods had wider confident prediction range compared with Delany-Bazley method.[21, 25,26] Thus, the predicted and measured impedance absorption coefficients was also compared in this paper in the frequency range of 200 - 4200 Hz.

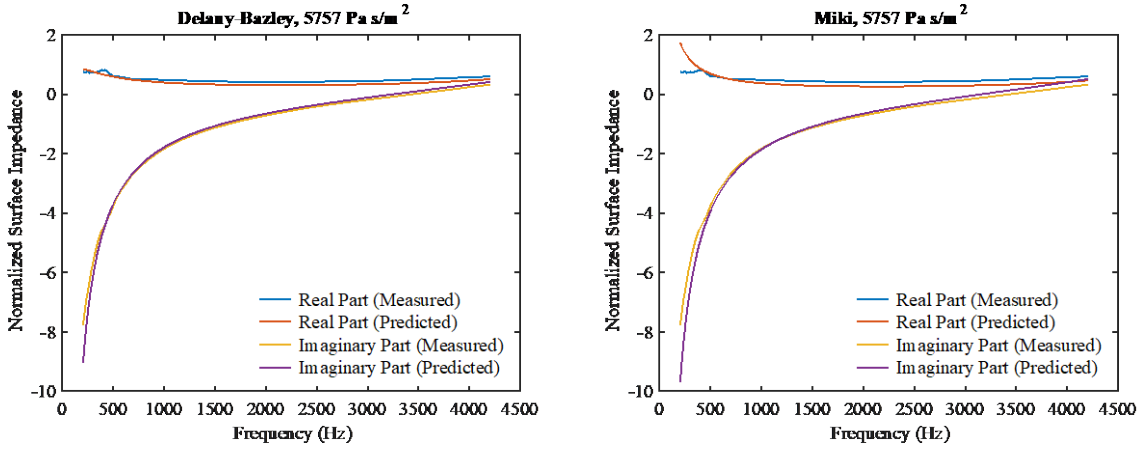

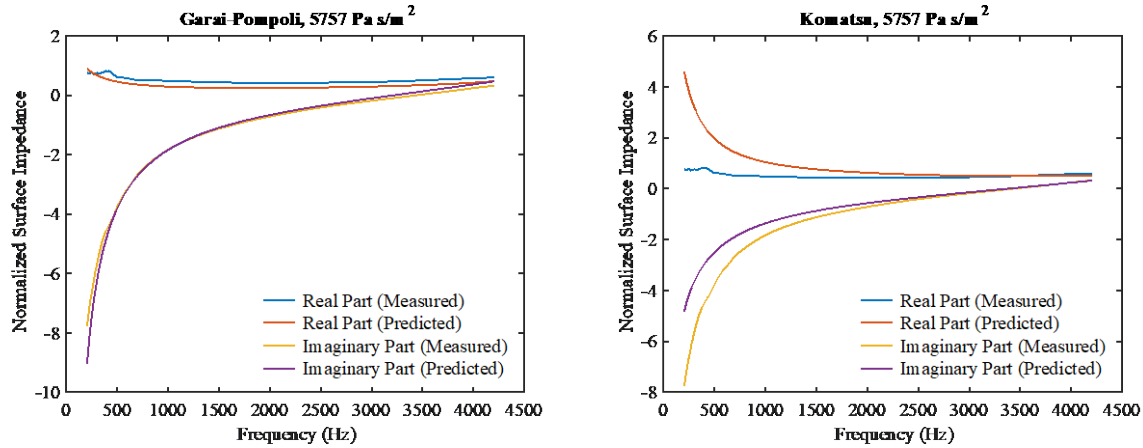

Figure 8. Measured and predicted impedance for the sample with airflow resistivity of 5757 Pa s/m².

One sample of WM20 type nonwoven with 5757 Pa·s/m² airflow resistivity was chosen to determine the most suitable model for impedance prediction of multi-component polyester nonwoven. Figure 8 demonstrates the comparisons of normalized impedance between the measured values and the values calculated using the Delany–Bazley model, the Miki model, the Garai-Pompoli and the Komstsu model. The normalized surface impedance is the ratio of surface impedance to the characteristic impedance of air ($Z_s/\rho_0 c_0$). It can be seen that Delany-Bazley and Miki model have accurate predictions not only for the real part of the normalized surface impedance but also for the imaginary part, while Komatsu model exhibits significant difference compared to measured values especially at low to mid frequency range. The reason for the inaccuracy of Komatsu model can be attributed to a wider airflow resistivity range (i.e. 6000 - 72900 Pa s/m²) that was used to derive the impedance prediction equations that that used in this study (4108 to 20474 Pa·s/m²). The predictions of surface impedance for other types of nonwoven samples with varying airflow resistivity are presented in Appendix C.

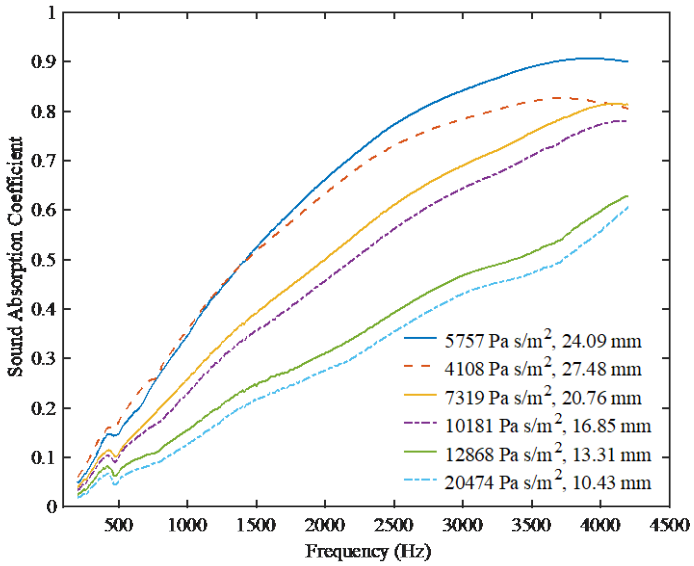

Figure 9. Sound absorption coefficient of polyester nonwoven samples with different airflow resistivity and thickness.

The absorption coefficient of six multi-component polyester nonwovens is shown in Figure 9. The airflow resistivity and thickness of each of these sample are also listed in the graph. The sound absorption results measured by impedance tube are plotted in the frequency range of 200-4200 Hz. As expected, the sample with the highest airflow resistivity and smallest thickness shows the lowest absorption coefficient in the whole measurement range. Meanwhile, the sample with 5757 Pa s/m² airflow resistivity and 24.09 mm thickness has the highest sound absorption performance in the mid- and high-frequency bands (i.e. 2000 – 4200 Hz). The thickest sample exhibits the best sound absorption capability at low-frequency band. It can be seen that the decrease of thickness results in decreasing of absorption coefficient at low-frequency band. This result is expected.[11, 35] The effect of airflow resistivity on sound absorption performance was also investigated in our previous study.[12] It was found that the sound absorption coefficient of fibrous materials with similar thickness increases with the increasing airflow resistivity up to around 6000 Pa s/m². After that the absorption coefficient decreases with the increase in airflow resistivity.[12, 36]

By applying predicted surface impedance into Eq. (2), the calculated absorption coefficient can be rapidly attained. A similar method for comparison between measured and predicted airflow resistivity was used to analyze the prediction errors of sound absorption coefficient among the four models. The relative prediction errors on sound absorption coefficient, δ_α, were calculated according to the following equation:

$$\delta_\alpha = \frac{|\sum \alpha_{meas} - \sum \alpha_{pred}|}{\sum \alpha_{meas}} \times 100\% \,, \tag{11}$$

where α_{meas} is the measured absorption coefficient, and α_{pred} is the predicted value.

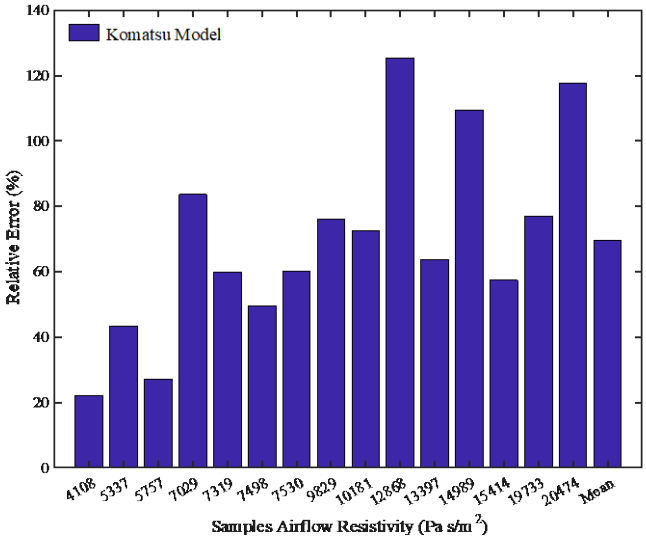

Figure 10. Relative prediction error based on Komatsu model. The airflow resistivity on horizontal axis represents corresponding samples.

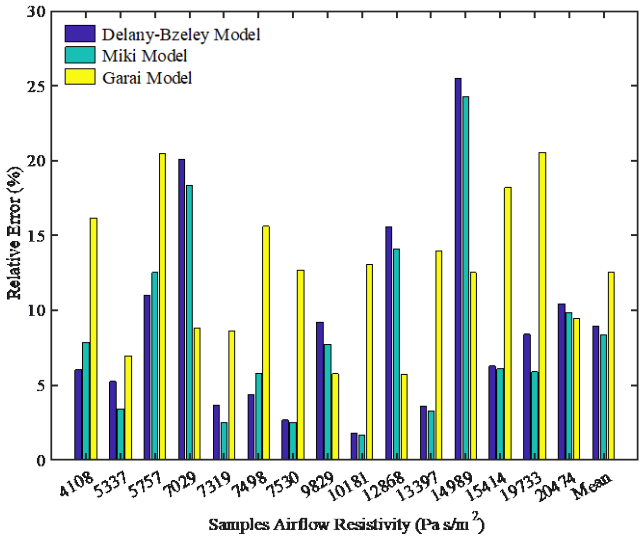

Figure 11. Relative prediction error based on Delany–Bazley model, Miki model and Garai-Pompoli model.

As shown in Figure 8 and Appendix C, the Komatsu model demonstrates the lowest accuracy in surface impedance prediction. Consequently, the error in the absorption coefficient based on Komatsu model can be very high as compared with that when predicted with the Delany-Bazley model and Miki model. In order to clearly show the adaptability of the models for multi-component polyester nonwovens, the prediction error with Komatsu model is separately presented in Figure 10. The errors in predictions with the Delany-Bazley, Miki and Garai-Pompoli models are shown in Figure 11. The Komatsu model exhibits the highest error of 125% for the sample with 12868 Pa s/m² airflow resistivity. This error is relatively low when the resistivity is small. The Komatsu method shows around 70% for its mean error, while the values from other three methods are less than 15%. From Figure 11 it is found that the Delany–Bazley and Miki models have similar accuracy. The difference in their mean errors is less than 0.6% which are 8.92% and 8.39%, respectively. It is found that the absorption coefficient predicted with the Miki model better prediction for a majority of the samples studied in this work than that achieved with the Delany-Bazley model. The errors between the Delany-Bazley and Miki models and measured values of the absorption coefficient are smaller than those between the Garai-Pompoli method and measured values. The maximum error of 25.48% is found between the absorption coefficient predicted by the Delany-Bazley model and that measured for the sample with 14989 Pa s/m² airflow resistivity. The maximum error in the Garai-Pompoli model is 20.57% for the sample with 19733 Pa s/m² airlow resistivity. The minimum errors achieved with the Delany-Bazley and Miki methods were 1.79% and 1.67%, respectively.

It can be considered that the results with an error less than 10% are accurate enough for this kind of analysis, as the value of bulk density and thickness for a fibrous material can vary due to several uncertainties during measurements. Uncertainties such as fabric compression, fiber density and any inaccuracy or noise that is present during the acquisition of the acoustical data might have resulted in erroneous data.[34] Thus, it can be concluded that the Delany-Bazley and

Miki models are superior in terms of the sound absorption coefficient when compared against the Garai-Pompoli and Komatsu models. It can also be concluded that the Miki model can be used to accurately predict sound absorption coefficient of multi-component polyester nonwovens.

Conclusion

This work studied the airflow resistivity, impedance and sound absorption properties of multi-component polyester nonwoven materials by using experimental and numerical methods. The samples made with three types of polyester fibers were chosen to carry out this study. The airflow resistivity and impedance tube measurements were well performed in the Jonas Lab at the University of Sheffield. The values of airflow resistivity were obtained through AFD300 AcoustiFlow device. Impedance and sound absorption coefficient measurements on some samples were conducted by using Materiacustica impedance tube. Six models based on capillary channel and drag force theories as well as empirical method were used to predict airflow resistivity. One simple empirical model based on the Nichols[21] method was proposed. The proposed empirical model demonstrates an error of 6.8% by simple using fiber diameter and nonwoven bulk density as input. The airflow resistivity results also indicated that one of the model proposed by Tarnow[20] exhibits the most suitable prediction with the relative error of 12.0%.

The Delany-Bazley, Miki, Garai-Pompoli and Komatsu models were applied to predict the acoustic properties. Subsequently, the measured and predicted values of the acoustical properties were compared to study their prediction accuracy. It was found that the Komatsu model is the least accurately predict the surface impedance, especially in the low-frequency range. The Delany-Bazley and Miki models showed a good agreement with the measured real and imaginary parts of the surface impedance. It was also observed that the Delany-Bazley and Miki models can accurately predict absorption coefficient for multi-component polyester nonwoven materials. Miki model exhibits the lowest mean relative error of 8.39%.

Declaration of conflicting interests

The authors declare no potential conflicts of interest with respect to the research, authorship, and/or publication of this article.

Acknowledgement

This work was supported by the research project of the Student Grant Competition of Technical University of Liberec no. 21239 granted by the Ministry of Education Youth and Sports of the Czech Republic, DENORMS Cost Action Short Term Scientific Mission funding scheme, European Structural and Investment Funds in the frames of Operational Programme Research, Development and Education – project Hybrid Materials for Hierarchical Structures (HyHi, Reg. No. CZ.02.1.01/0.0/0.0/16_019/0000843) and by project "Modular platform for autonomous chassis of specialized electric vehicles for freight and equipment transportation", Reg. No. CZ.02.1.01/0.0/0.0/16_025/0007293. The authors would like to thank Alistair I. Hurrel and Mohan Jiao for their help throughout the airflow resistivity and impedance tube measurements.

Appendix A. Summary of the formula from the impedance models

Delany-Bazley model:

$$Z_c = \rho_0 c_0 \left(1 + 0.0571 \left(\frac{\rho_0 f}{\sigma}\right)^{-0.754} - j0.087 \left(\frac{\rho_0 f}{\sigma}\right)^{-0.732}\right) \quad \text{(A1)}$$

$$k = \frac{\omega}{c_0}\left(0.189 \left(\frac{\rho_0 f}{\sigma}\right)^{-0.595} + j\left(1 + 0.0978 \left(\frac{\rho_0 f}{\sigma}\right)^{-0.7}\right)\right), \quad \text{(A2)}$$

where σ is the airflow resistivity, f is the frequency, $j = \sqrt{-1}$ is the complex number and $\omega = 2\pi f$ is the angular frequency.

Miki model:

$$Z_c = \rho_0 c_0 \left(1 + 0.0699 \left(\frac{f}{\sigma}\right)^{-0.632} - j0.107 \left(\frac{f}{\sigma}\right)^{-0.632}\right) \quad \text{(A3)}$$

$$k = \frac{\omega}{c_0}\left(0.160 \left(\frac{f}{\sigma}\right)^{-0.618} + j\left(1 + 0.109 \left(\frac{f}{\sigma}\right)^{-0.618}\right)\right). \quad \text{(A4)}$$

Garai-Pompoli model:

$$Z_c = \rho_0 c_0 \left(1 + 0.078 \left(\frac{\rho_0 f}{\sigma}\right)^{-0.623} - j0.074 \left(\frac{\rho_0 f}{\sigma}\right)^{-0.660}\right) \quad \text{(A5)}$$

$$k = \frac{\omega}{c_0}\left(0.159 \left(\frac{\rho_0 f}{\sigma}\right)^{-0.571} + j\left(1 + 0.121 \left(\frac{\rho_0 f}{\sigma}\right)^{-0.530}\right)\right). \quad \text{(A6)}$$

Komatsu model:

$$Z_c = \rho_0 c_0 \left(1 + 0.00027 \left(2 - \log\frac{f}{\sigma}\right)^{6.2} - j0.0047 \left(2 - \log\frac{f}{\sigma}\right)^{4.1}\right) \quad \text{(A7)}$$

$$k = \frac{\omega}{c_0}\left(0.0069 \left(2 - \log\frac{f}{\sigma}\right)^{4.1} + j\left(1 + 0.0004 \left(2 - \log\frac{f}{\sigma}\right)^{6.2}\right)\right). \quad \text{(A8)}$$

Appendix B. The values of airflow resistivity

Table B1. The predicted and measured airflow resistivity.

Samples	Bulk density (kg/m^3)	Kozeny-Carman	Pelegrinis et al.	Langmuir	Tarnow	Garai - Pompoli	Manning - Panneton	Fitted	Measured
		Airflow Resistivity ($Pa \cdot s/m^2$)							
WM20	21.07	4711	4455	8485	5842	8043	7750	6219	5757 ± 589
WM20	24.45	6401	5998	10435	7138	9911	9710	7849	7319 ± 243
WM20	26.71	7611	7161	11821	8052	11223	11105	9016	7530 ± 408
WM20	27.54	8189	7611	12343	8394	11714	11630	9456	9829 ± 376
WM20	35.56	13960	12695	17840	11962	16776	17139	14112	14989 ± 285
WM20	35.87	14209	12912	18062	12105	16976	17359	14300	15414 ± 167
WM20	45.56	23538	20832	25777	17005	23750	24944	20791	19733 ± 433
ST G1	23.54	5920	5562	9898	6782	9398	9169	7398	7498 ± 332
ST G1	30.94	10433	9608	14577	9853	13795	13876	11347	13297 ± 277
ST G2	16.93	3008	2877	6292	4370	5917	5564	4416	4108 ± 199
ST G2	19.49	4015	3813	7623	5266	7210	6887	5505	5337 ± 217
ST G2	22.48	5387	5075	9286	6376	8813	8554	6886	7029 ± 356
ST G2	27.61	8234	7651	12389	8424	11757	11676	9495	10181 ± 259
ST G2	34.95	13461	12262	17840	11575	16372	16694	13734	12868 ± 199
ST G2	44.60	22504	19969	24976	16495	23055	24157	20114	20474 ± 687

Appendix C. Predictions of surface impedance for the nonwoven samples with varying airflow resistivities

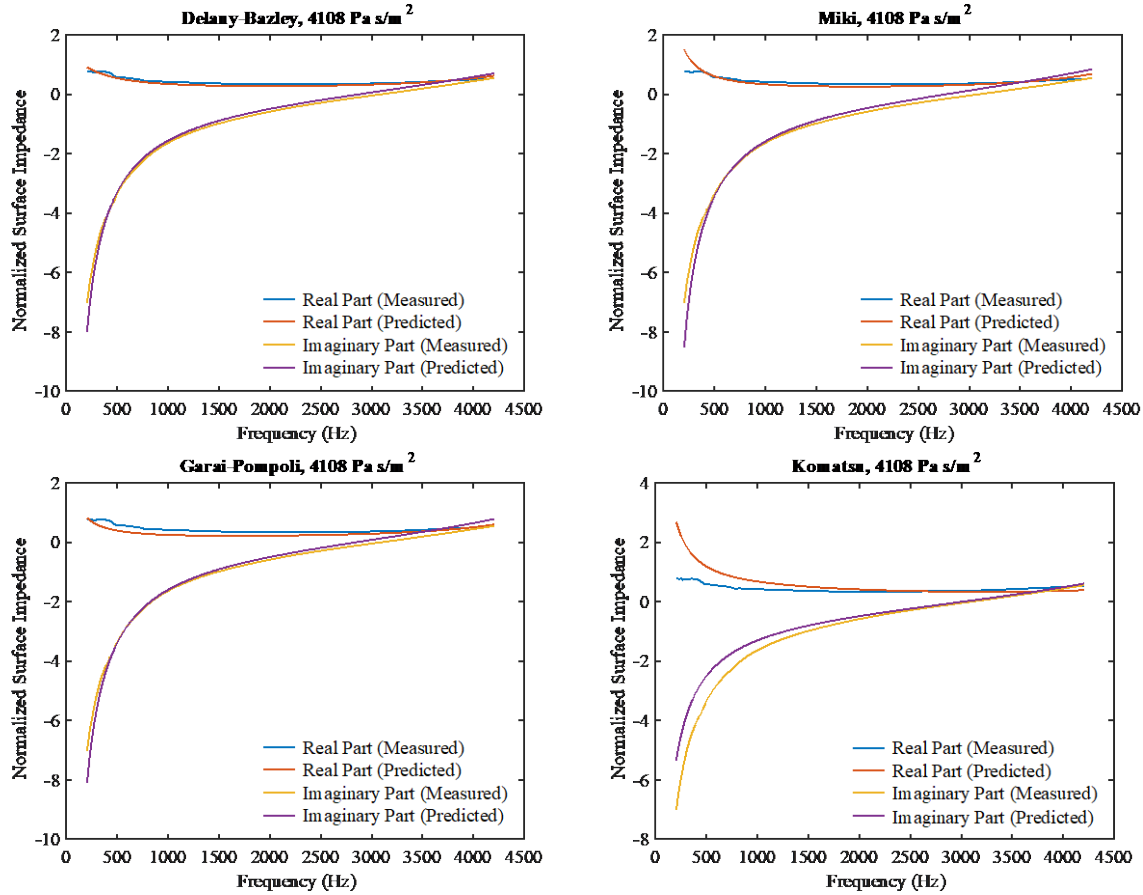

Figure C1. Measured and predicted impedance for the sample with airflow resistivity of 4108 Pa·s/m².

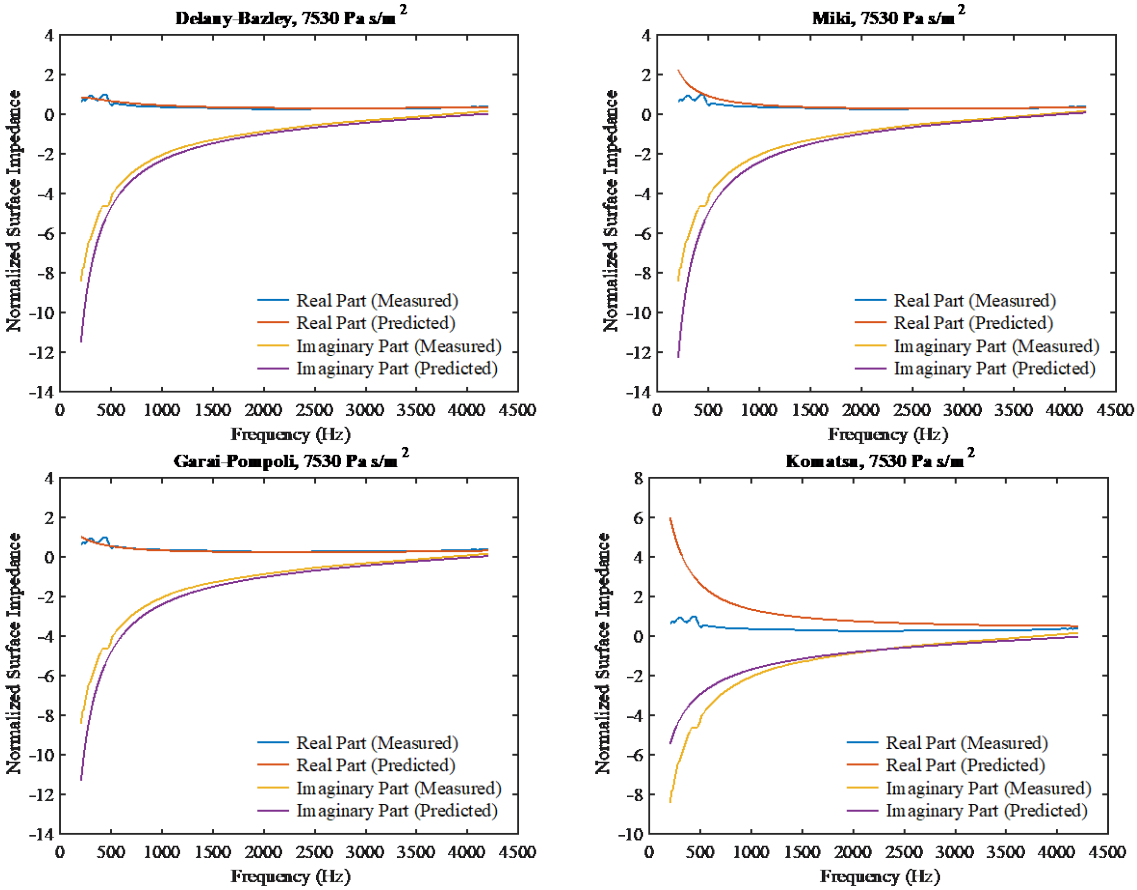

Figure C2. Measured and predicted impedance for the sample with airflow resistivity of 7530 Pa·s/m².

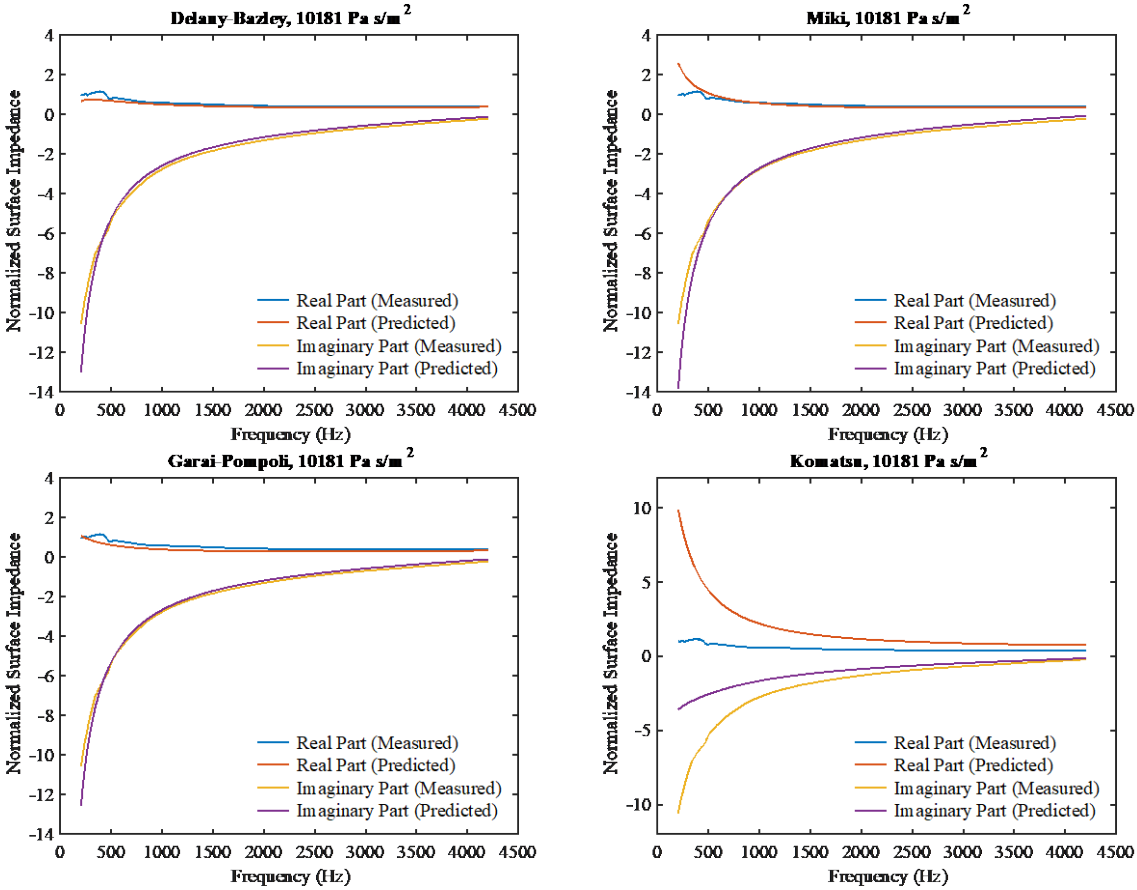

Figure C3. Measured and predicted impedance for the sample with airflow resistivity of 10181 Pa·s/m².

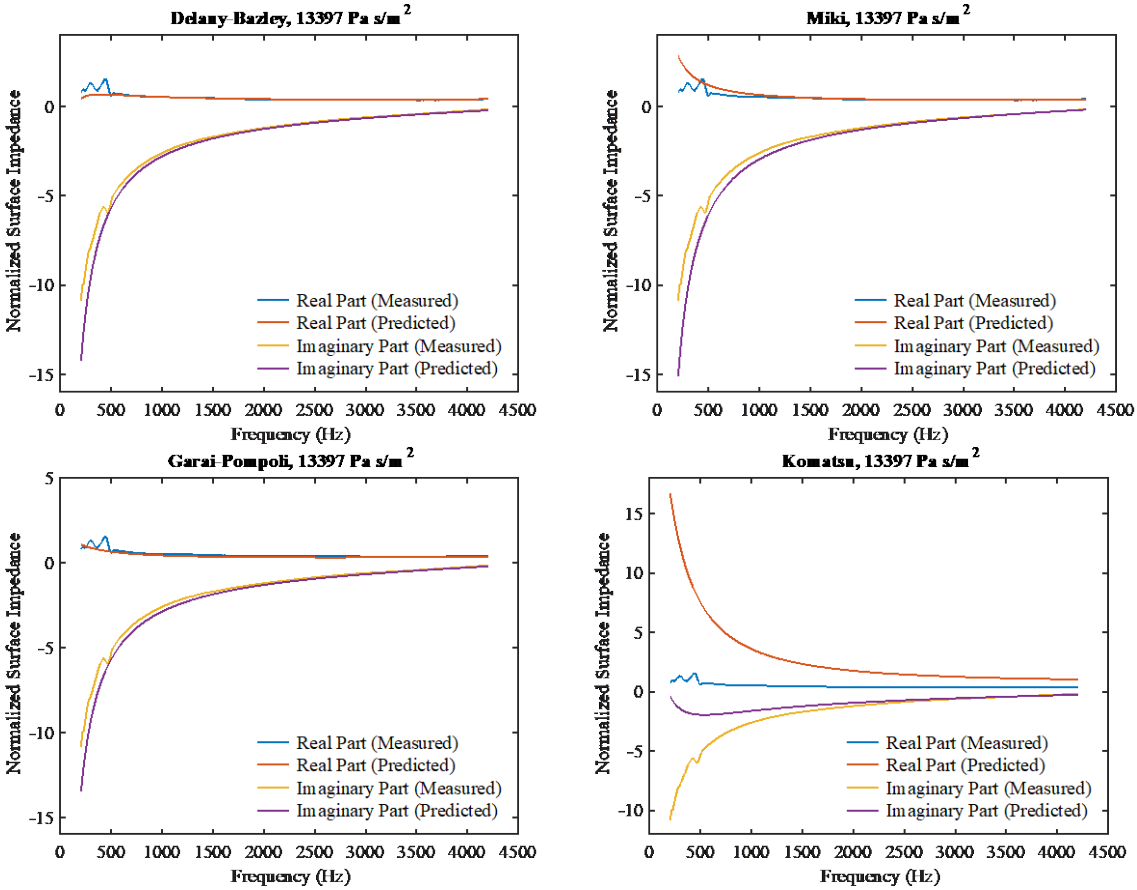

Figure C4. Measured and predicted impedance for the sample with airflow resistivity of 13397 Pa·s/m².

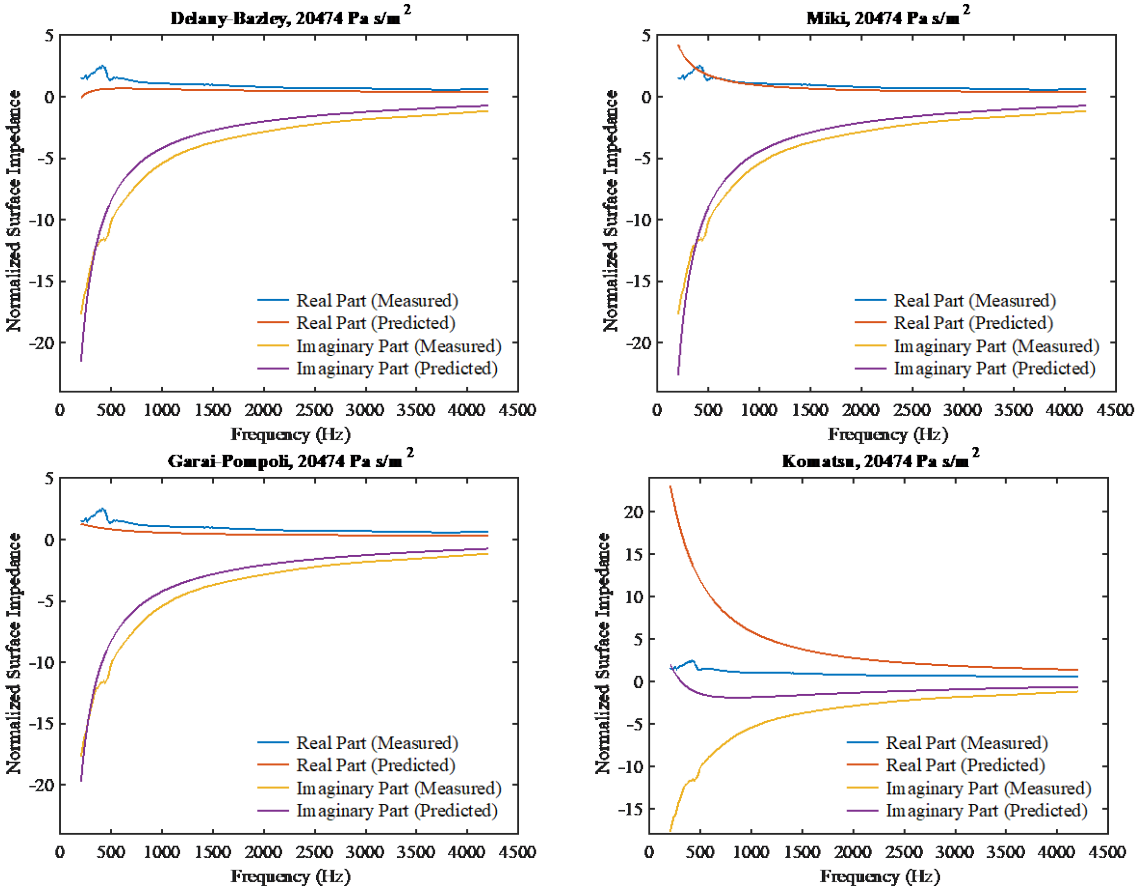

Figure C5. Measured and predicted impedance for the sample with airflow resistivity of 20474 Pa·s/m².

Reference:

1. Cox TJ and D'Antonio P. *Acoustic Absorbers and Diffusers: Theory, Design and Application*. 2nd ed. London; New York: Taylor & Francis, 2009, p. 156-157.

2. Albrecht W, Fuchs H and Kittelmann W. *Nonwoven fabrics*. Weinheim: Wiley-VCH, 2003, p.748.

3. Wang CN and Torng JH. Experimental Study of the Absorption Characteristics of Some Porous Fibrous Materials. *Appl Acoust* 2001; 4: 447–459.

4. Chen Y and Jiang N. Carbonized and Activated Non-Wovens as High-Performance Acoustic Materials: Part I Noise Absorption. *Text Res J* 2007; 77: 785–791.

5. European Council Directive 67/548/EEC of 27 June 1967, On the approximation of laws, regulations and administrative provisions relating to the classification, packaging and labelling of dangerous substances, *Official Journal of the European Union* 1967; 196: 1-98.

6. Mamtaz H, Fouladi MH, Al-Atabi M and Namasivayam SN. Acoustic Absorption of Natural Fiber Composites. *Journal of Engineering* 2016; 2016: 1-11.

7. Tang X and Yan X. Acoustic energy absorption properties of fibrous materials: A review. *Composites Part A* 2017; 101: 360-380.

8. Thilagavathi G, Pradeep E, Kannaian T and Sasikala L. Development of Natural Fiber Nonwovens for Application as Car Interiors for Noise Control. *J Ind Text* 2010; 39: 267–278.

9. Oldham DJ, Egan CA and Cookson RD. Sustainable Acoustic Absorbers from the Biomass. *Appl Acoust* 2011; 72: 350–363.

10. Pelegrinis MT, Horoshenkov KV and Burnett A. An Application of Kozeny–Carman Flow Resistivity Model to Predict the Acoustical Properties of Polyester Fibre. *Appl Acoust* 2016; 101: 1–4.

11. Yang T, Xiong X, Mishra R, Novak J and Militky J. Acoustic evaluation of Struto nonwovens and their relationship with thermal properties. *Text Res J* 2018; 88: 426–437.

12. Yang T, Xiong X, Mishra R, Novák J, Militký J. Sound absorption and compression properties of perpendicular-laid nonwovens. *Text Res J* 2018. doi: 10. 1177/0040517517753634.

13. Tascan M and Vaughn EA. Effects of fiber denier, fiber cross-sectional shape and fabric density on acoustical behavior of vertically lapped nonwoven fabrics. *J Eng Fiber Fabr* 2008; 3: 32–38.

14. Xue Y, Bolton JS, Gerdes R, Lee S and Herdtle T. Prediction of Airflow Resistivity of Fibrous Acoustical Media Having Two Fiber Components and a Distribution of Fiber Radii. *Appl Acoust* 2018; 134: 145–153.

15. Zwikker C and Kosten CW. Sound Absorbing Materials. New York: Elsevier: 1949.

16. Yang T, Mishra R, Horoshenkov KV, Hurrell A, Saati F and Xiong X. A Study of Some Airflow Resistivity Models for Multi-Component Polyester Fiber Assembly. *Appl Acoust* 2018; 139 139: 75–81.

17. Carman PC. Flow of Gases through Porous Media. New York: Academic Press, 1956.

18. Scheidegger AE. THE PHYSICS OF FLOW THROUGH POROUS MEDIA, Adrian E.: University of Toronto Press, Toronto Hardcover, 2nd Edition, 1963.

19. Jackson GW and James DF. The Permeability of Fibrous Porous Media. *Can J Chem Eng* 1986; 64: 364–374.

20. Tarnow V. Airflow Resistivity of Models of Fibrous Acoustic Materials. *J Acoust Soc Am* 1996; 100: 3706–3713.

21. Nichols RH. Flow-Resistance Characteristics of Fibrous Acoustical Materials. *J Acoust Soc Am* 1947;19: 866–871.

22. Garai M and Pompoli F. A Simple Empirical Model of Polyester Fibre Materials for Acoustical Applications. *Appl Acoust* 2005; 66: 1383–1398.

23. Manning J and Panneton R. Acoustical Model for Shoddy-Based Fiber Sound Absorbers. *Text Res J* 2013; 83: 1356–1370.

24. Delany ME and Bazley EN. Acoustical Properties of Fibrous Absorbent Materials. *Appl Acoust* 1970; 3: 105–116.

25. Miki Y. Acoustical Properties of Porous Materials-Modifications of Delany-Bazley Models. *Journal of the Acoustical Society of Japan (E)* 1990; 11: 19–24.

26. Komatsu T. Improvement of the Delany-Bazley and Miki Models for Fibrous Sound-Absorbing Materials. *Acoust Sci & Tech* 2008; 29: 121-129.

27. Jirsak O and Wadsworth L. Nonwoven Textiles. Durham, NC: Carolina Academic Pr, 1998.

28. ASTM C830-00: 2000. Standard test methods for apparent porosity, liquid absorption, apparent specific gravity, and bulk density of refractory shapes by vacuum pressure.

29. Maciel N de OR, Ribeiro CGD, Ferreira J, Vieira J da S, Marciano CR, Vieira CM, Margem FM and Monteiro SN. Comparative Analysis of Curaua Fiber Density Using the Geometric Characterization and Pycnometry Technique. In: Ikhmayies S, Li B, Carpenter JS, et al., eds. *Characterization of Minerals, Metals, and Materials 2017*. Cham: Springer International Publishing; 2017:11-19.

30. McRae JD, Naguib HE and Atalla N. Mechanical and Acoustic Performance of Compression-Molded Open-Cell Polypropylene Foams. *J Appl Polym Sci* 2010; 116: 1106–1115.

31. ISO 9073-1:1989. Textiles -- Test methods for nonwovens -- Part 1: Determination of mass per unit area.

32. ISO 9053-1991: Acoustics -- Materials for acoustical applications -- Determination of airflow resistance.

33. ISO10534-2:1998. Determination of sound absorption coefficient and impedance in impedance tubes, Part 2: Transfer-function method international organization for standardization.

34. Hurrell AI, Horoshenkov KV and Pelegrinis MT. The Accuracy of Some Models for the Airflow Resistivity of Nonwoven Materials. *Appl Acoust* 2018; 130: 230-237.

35. Coates M and Kierzkowski M. Acoustic textiles: lighter, thinner and more sound absorbent. *Tech Text Int* 2002; 11: 15–18.

36. Zent A and Long JT. Automotive sound absorbing material survey results. *SAE Int* 2007; 25: 1-7.